A Bistable Lightweight Gripper for Soft Manipulators

Johannes Frey*[1,2], Andrea Peirone*[3], Francesco Stella*[3], Cosimo Della Santina[4,5], Josie Hughes†[3] and Edoardo Milana †[1,2]

***Abstract*— Bistable soft grippers can maintain a grasp without continuous actuation, thereby reducing energy consumption. Furthermore, lightweight designs tailored to soft continuum manipulators are in high demand. This paper presents a 3D-printed, 114 g bistable gripper for the Helix soft continuum manipulator, achieved by integrating a modular dome-shaped snapping element in a flower-inspired TPU monolithic gripper. We design the bistable dome based on three geometric parameters: Inclination angle α, wall thickness s, and hole length l. To find a suitable design, we experimentally characterize seven designs via compression testing. The selected geometry ($s = 3$ mm, $\alpha = 75°$, $l = 14$ mm) maximizes the bistability and the resulting gripping force and has a 70 mm radial finger closing range. Mechanical characterization shows that the bistable gripper exerts a passive gripping force at zero actuation input, eliminating sustained motor torque during the hold phase. Grasping trials across eight objects demonstrate reliable grasping for objects up to 85 g and footprints between $40{\times}40$ mm and $75{\times}75$ mm without any actuation during holding. Comparison with a monostable counterpart shows that while the bistable gripper significantly reduces energy consumption during gripping, the monostable design has superior versatility for heavier and geometrically more diverse objects. These results establish clear design guidelines for integrating bistability into lightweight grippers for soft manipulators.**

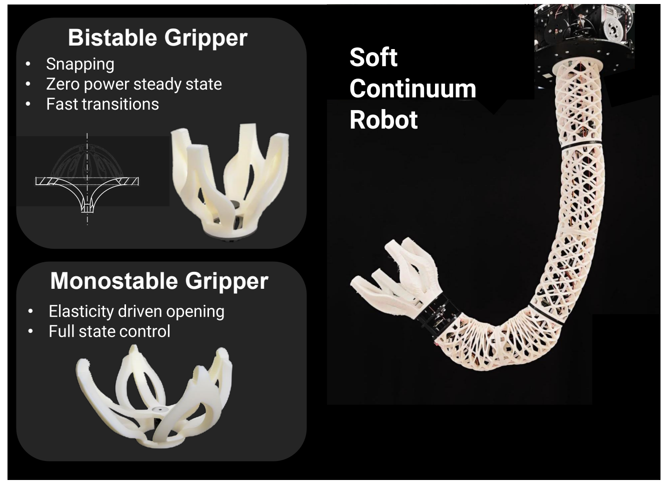

Fig. 1. Overview of the developed bistable gripper and the monostable design for comparison, together with its integration on the Helix soft continuum manipulator.

I. Introduction

The act of grasping objects is one of the most pervasive tasks in everyday life [1]. The ability of a soft robot to interact safely with the external environment makes these new technologies more suitable for systems that need to handle a large variety of objects. The capacity for deformation under minimal forces and the ability to adapt to diverse shapes and objects in response to external stimuli make soft robotics an optimal choice for the engineering of versatile compliant grippers [2], [3]. Another advantage of soft materials is the possibility to program their mechanical response by design. As soft materials undergo very large and reversible strains, nonlinear mechanical effects, which are typically catastrophic for rigid materials (e.g. buckling), can be leveraged to increase the functionality of soft robotic systems [4], [5]. Snapping and multistable structures are widely implemented in soft robots as a pathway towards physical control [6], given their nonlinear properties. Such structures may act as switches [7], amplifiers [4], and sequencers [8], since their mechanical response acts as force thresholds. To fully leverage the power of safe and adaptive manipulation, it is crucial to present new designs of soft, compliant grippers that have physical control capabilities and can be integrated into soft and safe manipulators, together with real-world testing of the full system, and consideration of the weight and adaptability requirements of soft continuum arms. Bistability is instrumental in grasping, for several reasons [9]. Firstly, it enables a grasp to be maintained without consuming power. Moreover, as the structure changes stable state with very fast snap-through movement, the gripper can also benefit from quick openings and closings, enabling highly dynamic grasping. Finally, bistability allows for simplified control, only regulating the timing of the state transition. Examples of bistable grippers in the literature leverage several mechanisms: Geometrical constraints in pre-stressed beams [10], dome-shaped structures [11]–[13], buckled beams [14], and shells [15]. Disadvantages include that the gripper can assume only two configurations, preventing the successful grasping of objects that are geometrically incompatible with the "closed" state. In this work, we integrate bistable capabilities in a soft gripper designed for the Helix robot [16], [17]. As such, the gripper must fulfill precise re-

This work was funded by the Deutsche Forschungsgemeinschaft (DFG, German Research Foundation) under Germany's Excellence Strategy-EXC-2193/1-390951807 and Horizon Europe Program from Project EMERGE grant agreement N° 101070918. Milana and Stella are grateful to the Freiburg Rising Stars Academy for enabling this collaboration.

*Equally contributing first authors. †Equally contributing last authors.

[1]Department of Microsystems Engineering - IMTEK, University of Freiburg, Freiburg, Germany. [2]livMatS@FIT, University of Freiburg, Freiburg, Germany. [3]CREATE Lab, EPFL, Lausanne, Switzerland. [4]Department of Cognitive Robotics, Delft University of Technology, Delft, The Netherlands. [5]Institute of Robotics and Mechatronics, German Aerospace Center (DLR), Wessling, Germany. Contact emails: edoardo.milana@imtek.uni-freiburg.de, josie.hughes@epfl.ch.

quirements in terms of size, weight, and actuation mode. We give the Helix gripper bistable capabilities by adding a modular dome-shaped soft structure, therefore implementing a discrete control (”open” and ”closed” state). To develop the bistable gripper, we parametrize and characterize a new class of dome-shaped bistable elements, and we present the experimental analysis to find a trade-off suitable for the gripper. To summarize, this paper contributes to the state of the art in the design and characterization of a bistable soft gripper that is based on a snap-through element. In particular, we present

- the parametric design and experimental analysis of a bistable, compliant gripper,
- an experimental validation of the grasping performance across objects of varying weight and geometry,
- a force comparison between the bistable and monostable grippers, and a brief demonstration of the bistable gripper mounted on the Helix soft continuum arm.

II. Design & Methods

In the following section, we introduce the methodology used to design the bistable gripper. First, we introduce the bistable element, its parametric design and how it is integrated. We then present the differences to a comparable monostable gripper, before introducing the experiments used to compare and analyse the grippers.

A. Design and analysis of the bistable element

Inspired by a mechanical cup spring, we propose a bistable design with two stable states, as depicted in Fig. 2A: The natural state (global energy minimum) and the metastable snapped state (local energy minimum). This enables us to build a gripper with a low actuation force to close and a higher one to open, ensuring a stable grasp while minimizing energy consumption. Figure 2B shows the geometry of the bistable dome, which is characterized by the geometrical design parameters: The angle of inclination α, the thickness s at the central line, and the length l of the drop-shaped holes. The inclination angle α of the dome surface is defined between the tangent to the dome at its rim and the base plane. The length l of the 12 drop-shaped holes is evaluated according to the design parameters to make the hole tangent to the junction and allow the structure to snap. In the deformed configuration, the gap between these holes closes as the two sides get into contact. The diameter of the snapping element matches the diameter of the manipulator. The central hole acts as a mounting point for the actuation mechanism of the gripper. To find a suitable geometry of the bistable snapping element, we determine the force-displacement curves of a set of 7 bistable elements with different design parameters s and α. The set of samples is FDM-3D printed using a Prusa MK4 printer and TPU filament with a Young's Modulus of 40 MPa and an ultimate elongation of 475%. [17]. For printing, we use 100% infill, a nozzle temperature of 235 °C, a bed temperature of 30 °C, a layer height of 0.15 mm, and a print speed of 60 mm/s. To obtain the force-displacement curves and identify the stable states, compression tests are carried out with a Zwick Roell Z010 machine with a maximum test load of 10 kN and a sensitivity of 1 mN (see Figure 5). During the experiment, the starting position is identified via force feedback, with a minimum force threshold set at 0.1 N. Subsequently, the structure is compressed at a constant speed of 0.5 mm/s to test the system in quasi-static equilibrium conditions. We measure the peak and valley points of the actuation-force-displacement curves to compare the samples quantitatively.

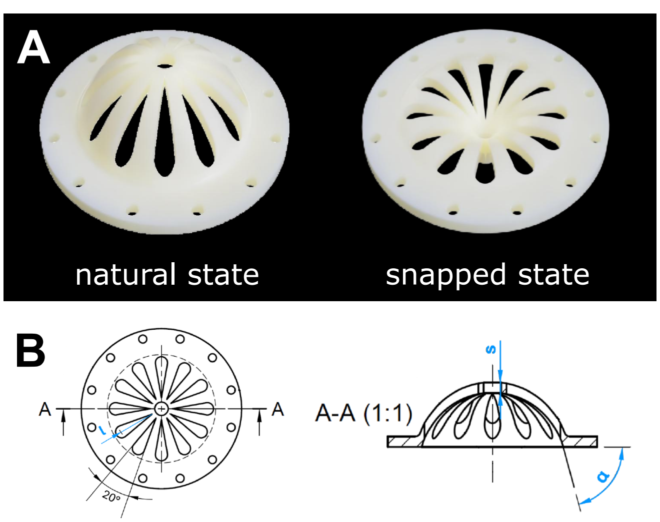

Fig. 2. (A) The 3D-printed, dome-shaped snapping element in natural and snapped states. (B) Technical drawing of the snapping element with its design parameters (blue).

B. Gripper design, fabrication, and characterization

The gripper is designed to safely and effectively handle fragile and irregularly shaped objects, ensuring high flexibility and control during gripping operations. The design is inspired by flowers and consists of a monolithic main body that integrates 4 fingers. The working principle is based on the vertical actuation of the horizontal base of the gripper, where the fingers are attached. This movement causes the gripper to close. In recent work, a version with integrated fluidic sensing of the same gripper was introduced [18]. The gripper is 3D-printed from TPU with NinjaFlex Filament 85A (Young's Modulus $E = 4$ MPa, ultimate elongation 660%). We print the gripper with a nozzle temperature of 235 °C, a bed temperature of 30 °C, a layer height of 0.1 mm, a print speed of 30 mm/s, and 20% infill. These parameters ensure high compliance with the structural requirements and guarantee lightweight construction, which is a crucial feature for this application, given the payload limitations of the soft manipulator. Bistability is introduced by integrating the snapping element (see Figure 3). For maximum closing force of the gripper, the bistable element is in the natural state when the gripper is closed and in the metastable state when opened. The open gripper inscribes a circle with a diameter of 90 mm, which determines the maximum size of objects that can be grasped. The bistable structure is controlled via antagonistic tendons. The fingertips are grooved to provide

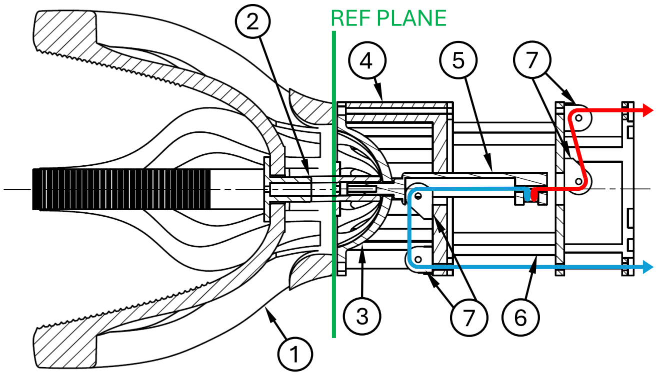

Fig. 3. Components of the bistable gripper assembly.

a firmer grip on the object being held, thereby ensuring a more stable and secure hold. The total weight of the gripper assembly is 114 g. Figure 3 shows the gripper (1) and its actuation mechanism with the bistable element (3) in the natural (stable) state, where it lies to the right of the reference plane. In contrast, if deformed into the snapped (metastable) state, as shown in Figure 2A, it lies to the left of the reference plane. The actuation tendons, displayed in red and blue, are routed through the gripper assembly via pulleys (7). They traverse the manipulator and connect to a servo-motor (Dynamixel XM430-W210-R), which is located in the robot base together with the motors that drive the robot. The gripper tendons are not coupled to the actuation of the manipulator and do not influence or restrict its motion. They are connected to the bistable element via the actuation rod (5), which connects to the gripper via a cap (2). Additional mounting elements (4, 6) connect the individual parts to form the gripper assembly. In the illustrated configuration, the actuation of the blue tendon results in the rod moving to the left, which causes the bistable element to snap, opening the gripper. Conversely, to close the gripper, the red tendon is actuated and returned to the configuration depicted. Once the gripper is closed, the red tendon can be released, as the bistability of the snapping element ensures that the closing force on the object is maintained without the need for actuation. The displacement of the rod and the bistable element has to be considered in the geometry of the gripper as it defines its range of motion. We assessed the performance of the bistable gripper against a monostable version of the design, which does not feature the bistable snapping element. Due to its inherent compliance, the monostable gripper naturally tends to the open state, and a tendon attached to the central element triggers its radial closing. The closed state is maintained at the cost of a constant torque applied by the motor via the tendon. When the tendon is released, the compliant structure opens passively. For grasping an object in the monostable version, the compliance of the gripper allows for simple position control of the motor. This way, objects are grasped with the stall torque of the motor. For a Dynamixel XM430-W210-R, the stall torque is 3 Nm at 2.3 A, and 12 V [19]. The electric energy consumption at stall torque can thus be determined by $\Delta E = \int_0^{\Delta t} UIdt$, where ΔE is the electric energy consumption, Δt is the gripping time, U is the supply voltage and I is the current at stall moment. In the bistable version, the motors provide only torque pulses to switch between states, while the objects are held passively by the compliance of the gripper. Thus, the energy consumption depends on the gripping time, as depicted in Figure 4. To characterize the mechanical response of the two gripper versions, we mount them on a tensile testing machine (ZwickRoell zwickiLine). To measure the actuation force required to close the grippers, we clamp the horizontal base of the gripper to the machine and pull it to displace it by 15 mm at a constant speed of 80 mm/min. The same displacement is applied in the opposite direction to open the gripper. We carry out the experiment three times with four cycles each for both gripper versions. In parallel, we place a load cell (max 50 N) next to a fingertip in the open gripper state (see Fig. 6C) to measure the gripping force exerted by one finger during these cyclic experiments. This way, the gripping force builds up right from the start of the experiment, matching an object whose size is equal to the maximum opening of the gripper. Hence, the experiment provides the maximum gripping force, which is characterized by the compliance of the gripper and the interaction with the object.

III. Results

In the following, we present results on the bistable snapping element characterization and the validation of the bistable gripper design and performance.

A. Characterization of the bistable snapping element

Table I summarizes the parameters of all tested snapping element samples and the related results of the compression test (peak and valley points of the actuation force F_A). These key values map directly to functional gripper properties, i.e., the relative closing of the fingers and the maximum gripping force. The peak and valley points correspond to the actuation force required to snap the bistable element between its two states. In a purely elastic structure, the valley point would lie in the negative-force region; however, in viscoelastic structures, the curve may cross zero force only during unloading. Nevertheless, the valley point measured

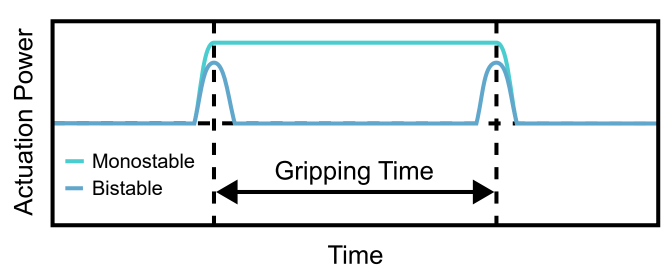

Fig. 4. Conceptual figure showing the advantages of integrating bistable elements in grippers. Bistability allows energy to be supplied only during the transition between open and closed states, saving the constant energy that a traditional monostable design requires throughout the gripping time.

TABLE I

ANALYSIS OF THE SNAPPING POINT OF DIFFERENT SNAPPING ELEMENT DESIGNS

	Geometrical Parameters			Valley Point		Peak Point	
Sample	s [mm]	α [°]	l [mm]	x[mm]	F_A[N]	x[mm]	F_A[N]
A	5	75	14.5	21.4	22.5	5.4	68.8
B	4	75	14.2	21.4	11.7	5.0	53.1
C	**3**	**75**	**14**	**19.2**	**1.8**	**4.0**	**29.1**
D	3	60	12	13.0	7.7	3.8	42
E	3	70	13.5	18.7	10.7	4.1	39.8
F	3	80	14.5	20.8	7.7	5.1	31.5
G	3	90	15	28.4	6.9	5.8	27.3

TABLE II

COMPARISON OF SUCCESSFUL GRASPS BETWEEN THE TWO GRIPPERS FOR OBJECTS OF VARYING WEIGHT AND DIMENSIONS

Object	Width×Depth×Height [mm]	Weight [g]	Bistable	Monostable
Tomatoes	40 x 40 x 20	35.6	Yes	Yes
Strawberries	30 x 10 x 10	19.6	No	Yes
Lemon	70 x 50 x 50	85.3	Yes	Yes
Water bottle	70 x 70 x 220	597.8	No	Yes
PLA cube 1	50 x 50 x 50	16.9	Yes	Yes
PLA cube 2	75 x 75 x 75	38.1	Yes	Yes
½ kg weight	99 x 99 x 15	500.1	No	Yes
Spacemouse Joystick	77 x 77 x 55	439.6	No	No

during loading provides a useful indicator of how pronounced the bistable effect is. Figure 5 shows an extract of the experimental results on the mechanical characterization of different bistable snapping element designs (D-G) with the same thickness s but varied angle α from 60° to 90°. The force-displacement curves of these structures show that the maximum force required to actuate the element decreases with increasing angle α. At the same time, the required force at the valley point is not significantly affected by the change of angle α. However, the curves show that increasing α leads to a larger compression stroke. This is due to the height of the domes, which increases with larger angles α. Bistability of the samples can be observed as the force-displacement curves cross zero during unloading. Note that at this point, the negative force exerted by the bistable dome cannot be captured with the compression test setup, as the dome loses contact with the machine. However, as mentioned, the hysteresis caused by the viscoelastic behaviour of TPU is clearly visible in the plots and results in the zero-crossing and thus the bistability of the samples. For samples A-C, angle α was kept constant, while the thickness parameter s was varied from 3 to 5 mm. Here, the results show that larger thickness s leads to higher forces at both peak and valley points, while the displacement is only marginally affected. This is because the the height of the dome does not change significantly with variation of parameter s. As a result of the parametric design search, we select the geometrical parameters $s = 3\,\text{mm}$, $\alpha = 75°$, $l = 14\,\text{mm}$ (sample C) as the best candidate among the tested samples for the final gripper design. We choose this design as it leads to the lowest actuation force at the valley point, matching the actuation system of the Helix manipulator and maximizing the bistability, hence the passive gripping it can achieve through compliance. For this design, the related actuation stroke resulting from the height of the bistable element also matches the Helix manipulator requirements. Consequently, the selected design represents a balance between the competing features, resulting in a closed gripper with an open fingertip area of 2 cm^2 and a relative radial closing of 70 mm.

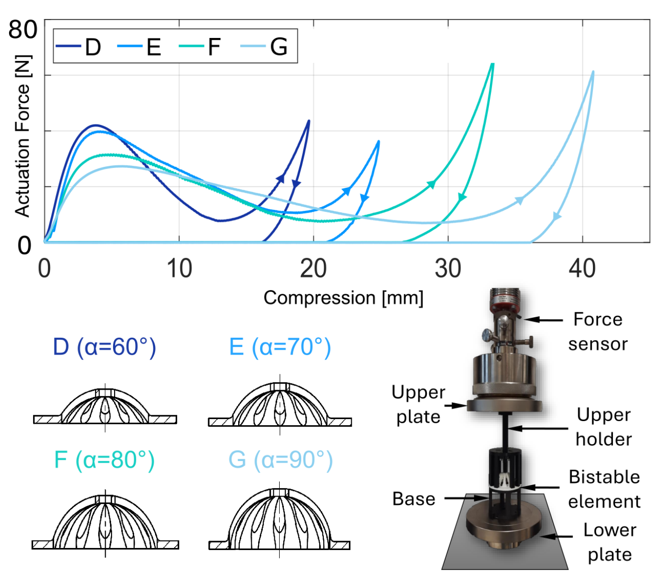

Fig. 5. Examples D, E, F, and G of bistable elements considered in the grid search presented in Table I. The response of the elements under compression (actuation force F_A) is measured using a Zwick Roell Z010 testing machine.

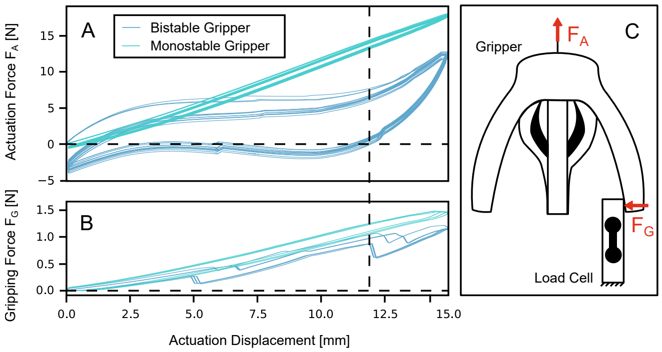

Fig. 6. Mechanical characterization of the bistable and monostable grippers. (A) Actuation force over displacement for the bistable (nonlinear, hysteretic) and monostable gripper; dashed lines indicate the snap-through transitions of the bistable gripper. (B) Gripping force over actuation displacement. The curves show the individual cycles of the experiment. (C) Sketch of the experimental setup.

B. Mechanical characterization of the gripper

The results of the mechanical gripper characterization are shown in Figure 6. The bistable gripper shows a very nonlinear, hysteretic force-displacement relationship, mostly dictated by the presence of the bistable element. The curve differs from the one of the element itself due to the coupling with the gripper's intrinsic elasticity. Nevertheless, the curve consistently crosses the zero-force line during unloading, showing the bistable behaviour of the gripper. Conversely, the monostable gripper shows a linear response with a minimal amount of hysteresis. As mentioned, this linearity enables continuous control of the gripper, but loses the zero-power states of the bistable configuration. The maximum gripping forces are depicted in subfigure B. When handling objects, the gripping force is a result of the compliance of the gripper interacting with the objects. The inherent compliance thus prevents damage to the objects. For both grippers, the gripping force increases linearly with the actuation, with the bistable one exhibiting some small force drops at the snapping points. It is important to notice how, for the bistable gripper, a gripping force is exerted even when the gripper is in the zero-force actuation point, which corresponds to the second stable state of the gripper. This shows that the gripping force results from the elastic force exerted by the gripper, and no actuation is needed, effectively inducing an important functionality. Regarding the Dynamixel motor used, holding an object with the monostable gripper at stall torque for 10 seconds, for example, would result in an energy consumption of 276 J. Neglecting the energy required to actuate the bistable dome, this is equivalent to the amount of energy that could be saved by using the bistable gripper for the same task.

C. Grasping capabilities

To benchmark the grasping capabilities of the two grippers, a thorough testing campaign is performed. During the testing, the grippers are connected to a fixed soft robotic arm, controlled to a stationary, vertical position. The grippers are tested on a variety of objects, with varying weights and sizes, to assess their capability across potential use cases. The objects are positioned on an adjustable-height plane, allowing for precise control over the initial grasping conditions. By adjusting the height of the plane, the test simulates different grasping scenarios, ensuring that the performance of the gripper is rigorously evaluated under consistent and repeatable conditions. This approach not only isolates the payload capacity of the grippers from the dynamics of the robotic arm but also provides a reliable framework for comparing the performance in handling various objects. The results, summarized in Table II and shown in Figure 7, display a higher overall success rate for the monostable gripper, while the bistable system achieves complete success for objects within its geometric compatibility range and up to 85 g. This geometric compatibility range corresponds to footprints between 40x40 mm and 75x75 mm. These results prove the efficiency of the bistable system for objects within the geometric compatibility range of the bistable gripper, with a good degree of adaptability of performance within the same class of objects, making the proposed bistable system a great solution for tasks that require holding objects for a long time. However, for a significantly varied group of objects to be manipulated, continuous actuation remains necessary, at the cost of a continuous energy supply. To illustrate the practical usability of the bistable gripper, we mount it on the Helix soft continuum manipulator [16] and demonstrate teleoperated manipulation in the supplemental video. Figure 8 shows snapshots from this demonstration.

IV. Discussion & Conclusion

In this work, we introduce a bistable, lightweight 3D-printed soft gripper tailored for the Helix robot manipulator by adding a dome-shaped snapping element to the opening mechanism of the gripper. The bistable gripper enables zero-

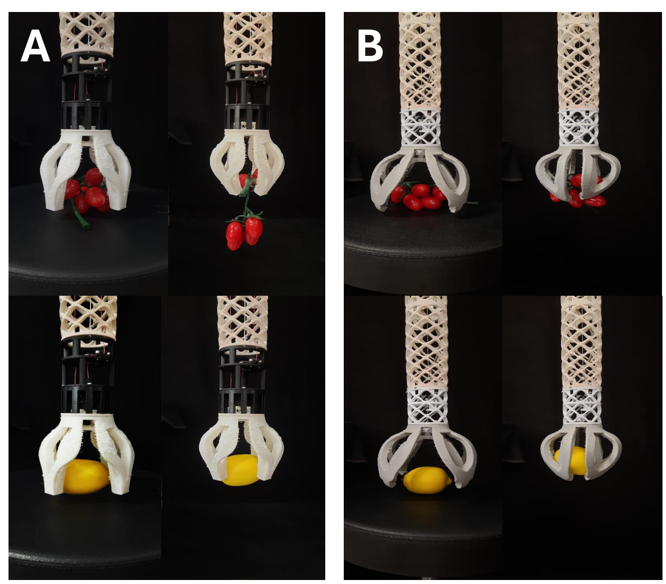

Fig. 7. Demonstration of the grasping capabilities of the soft grippers ((A) Bistable and (B) Monostable) when handling objects of diverse shape and weight, as detailed in Table II.

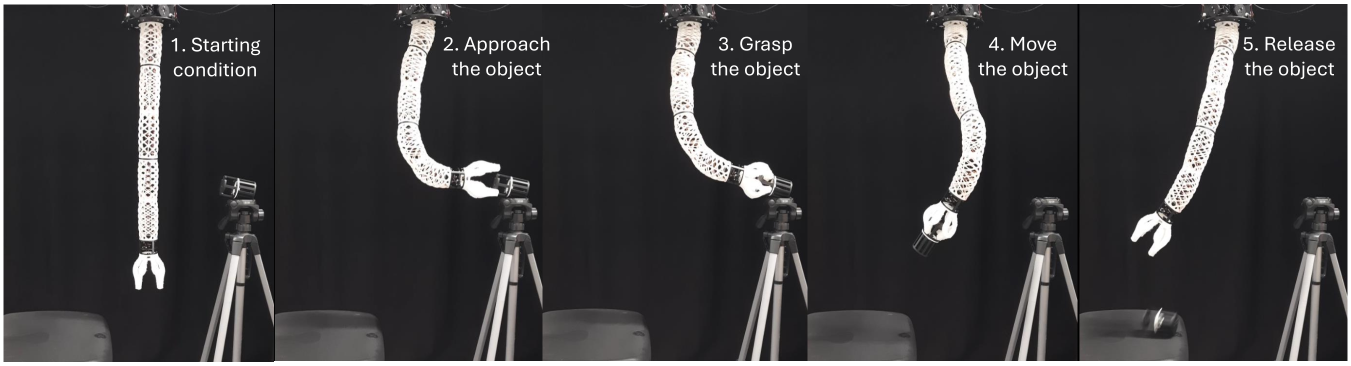

Fig. 8. Snapshots of the manipulation demonstration with the bistable gripper.

power gripping states and fast, snap-through actuation for a large range of objects. Integration with the Helix robot demonstrated the usability of the gripper in real-world tasks. However, compared to a conventional, monostable design, it offers less versatility in terms of object geometries and is limited to a characteristic gripping force by design. The bistable element was analysed and characterised experimentally. The selected design ($s = 3\,\text{mm}$, $\alpha = 75°$, $l = 14\,\text{mm}$) balances actuation force and displacement, and passive gripping force. In the bistable gripper, the resulting gripping force settles to the passive elastic equilibrium of the structure, avoiding a sustained actuation input. The gripping force in the bistable configuration is determined by the geometry of the snapping element, as well as its material properties. This means that the maximum gripping force is fixed for a given design. Experimental results confirm that the bistable gripper is better suited for applications where energy savings or fast release are priorities, and the object geometry is known. An exemplary application could involve manipulation of objects with UAVs, where robots pick up objects and carry them for a while before unloading. Here, the energy savings could significantly extend the operating time of the UAVs. However, the inherent limitations in terms of grasping versatility make monostable grippers preferable for a more diverse set of objects and applications with very frequent gripping, as found in pick-and-place scenarios, where energy savings might be marginal. Future work will further optimize the shape and geometry of the bistable element to augment the versatility of the objects that can securely be grasped.

References

[1] A. Bicchi and V. Kumar, "Robotic grasping and contact: A review," in *Proceedings 2000 ICRA. Millennium conference. IEEE international conference on robotics and automation. Symposia proceedings (Cat. No. 00CH37065)*, vol. 1. IEEE, 2000, pp. 348–353.

[2] J. Hughes, U. Culha, F. Giardina, F. Guenther, A. Rosendo, and F. Iida, "Soft manipulators and grippers: A review," *Frontiers in Robotics and AI*, vol. 3, p. 69, 2016.

[3] J. Shintake, V. Cacucciolo, D. Floreano, and H. Shea, "Soft robotic grippers," *Advanced materials*, vol. 30, no. 29, p. 1707035, 2018.

[4] J. T. Overvelde, T. Kloek, J. J. D'haen, and K. Bertoldi, "Amplifying the response of soft actuators by harnessing snap-through instabilities," *Proceedings of the National Academy of Sciences*, vol. 112, no. 35, pp. 10 863–10 868, 2015.

[5] E. De Smet, L. Migliorini, E. Milana, P. Milani, and B. Gorissen, "Electropneumatic oscillators using nonlinear inflatables," *Advanced Intelligent Systems*, p. 2400695, 2025.

[6] E. Milana, C. D. Santina, B. Gorissen, and P. Rothemund, "Physical control: A new avenue to achieve intelligence in soft robotics," *Science Robotics*, vol. 10, no. 102, p. eadw7660, May 2025. [Online]. Available: https://www.science.org/doi/10.1126/scirobotics.adw7660

[7] P. Rothemund, A. Ainla, L. Belding, D. J. Preston, S. Kurihara, Z. Suo, and G. M. Whitesides, "A soft, bistable valve for autonomous control of soft actuators," *Science Robotics*, vol. 3, no. 16, p. eaar7986, 2018.

[8] B. Van Raemdonck, E. Milana, M. De Volder, D. Reynaerts, and B. Gorissen, "Nonlinear inflatable actuators for distributed control in soft robots," *Advanced Materials*, vol. 35, no. 35, p. 2301487, 2023.

[9] Y. Chi, Y. Li, Y. Zhao, Y. Hong, Y. Tang, and J. Yin, "Bistable and multistable actuators for soft robots: Structures, materials, and functionalities," *Advanced Materials*, vol. 34, no. 19, p. 2110384, 2022.

[10] T. G. Thuruthel, S. H. Abidi, M. Cianchetti, C. Laschi, and E. Falotico, "A bistable soft gripper with mechanically embedded sensing and actuation for fast grasping," in *2020 29th IEEE International Conference on Robot and Human Interactive Communication (RO-MAN)*. IEEE, 2020, pp. 1049–1054.

[11] Q. Qi, C. Xiang, V. A. Ho, and J. Rossiter, "A sea-anemone-inspired, multifunctional, bistable gripper," *Soft Robotics*, vol. 9, no. 6, pp. 1040–1051, 2022.

[12] J. C. Osorio, J. S. Rincon, H. Morgan, and A. F. Arrieta, "Embodying control in soft multistable robots from morphofunctional co-design," *Advanced Science*, vol. 12, no. 32, p. e03206, 2025.

[13] H. Hanamori, A. Kawamura, and R. Kurazume, "Soft gripper driven by snap-through buckling for enveloping grasp," *ROBOMECH Journal*, vol. 13, 05 2026.

[14] H. de Souza Oliveira, X. Li, N. S. Khaanghah, N. Münzenrieder, and E. Milana, "Enabling proprioception in multistable soft machines through embedded soft capacitive sensors," *IEEE Journal on Flexible Electronics*, 2025.

[15] Z. Zhang, X. Ni, H. Wu, M. Sun, G. Bao, H. Wu, and S. Jiang, "Pneumatically actuated soft gripper with bistable structures," *Soft Robotics*, vol. 9, no. 1, pp. 57–71, 2022.

[16] Q. Guan, F. Stella, C. Della Santina, J. Leng, and J. Hughes, "Trimmed helicoids: an architectured soft structure yielding soft robots with high precision, large workspace, and compliant interactions," *npj Robotics*, vol. 1, no. 1, p. 4, 2023.

[17] F. Stella, G. Pei, O. Meebed, Q. Guan, Z. Bing, C. Della Santina, and J. Hughes, "Toward long-lasting large-scale soft robots: The durability challenge in architectured materials," in *2024 IEEE 7th International Conference on Soft Robotics (RoboSoft)*. IEEE, 2024, pp. 190–196.

[18] A. Zhang, H. Matusik, M. Flores-Acton, E. R. Sologuren, J. Jacob, and D. Rus, "Printed helicoids with embedded air channels make sensorized segments for soft continuum robots," in *2026 IEEE 9th International Conference on Soft Robotics (RoboSoft)*, Kanazawa, Japan, 2026.

[19] ROBOTIS. DYNAMIXEL XM430-W210-T/R E-Manual. Accessed: July 15, 2026. [Online]. Available: https://emanual.robotis.com/docs/en/dxl/x/xm430-w210/